

*Invited Paper***Terahertz holographic imaging using 3D-printed metasurfaces**

Jierong Cheng, Yiwu Yuan, Xipu Dong, Shengjiang Chang *
Nankai University, Institute of Modern Optics,
Tianjin Key Laboratory of Micro-Scale Optical Information Science and Technology,
38 Tongyan Rd, P. O. Box 300350, Tianjin, China
* Email: sjchang@nankai.edu.cn

(Received December 20, 2021)

Abstract: Metasurfaces significantly promote the development of holography by encoding the desired amplitude and phase modulation profile through subwavelength artificially designed resonators. Most of the dielectric metasurface holograms use high-index dielectric to avoid near field coupling. Here taking advantages of the diverse THz-transparent low-index polymers and the advanced 3D printing technique, we study the holographic imaging based on 3D-printed low-index metasurfaces. The phase hologram is calculated based on the Rayleigh-Sommerfeld diffraction theory and the Gerchberg-Saxton algorithm, which is implemented by polymer rods with varied dimensions and refractive index of 1.57. The simulation and consistent experimental results show that 3D-printed low-index dielectric metasurfaces offer a low-cost and time-saving scheme for wavefront transformation at terahertz frequencies.

Keywords: Terahertz, Hologram, Metasurface, 3D Printing, Refractive index

doi:

1. Introduction

The invention of holography [1, 2] offers a fascinating way to reconstruct 3D images and to achieve complicated wavefront shaping for information processing. Computer-generated holograms (CGHs) [3, 4] further revolutionize the holography by eliminating the recording process. Reconstruction of any object can be done by proper encoding of the numerically calculated phase information, which is usually done in surface relief structures [5] through phase accumulation. This conventional type of CGH has limitations of bulky size, low efficiency and low resolution.

Recently, metasurfaces provide a prevailing method for holographic imaging by encoding the desired amplitude and phase modulation into a thin layer of subwavelength-scale artificially designed resonators [6–8]. Taking advantages of the subwavelength feature size and the ultrathin thickness, metasurface holograms show increased resolution, enlarged field of view and improved efficiency. In 2015, a reflective metasurface hologram based on geometric phase scheme has been demonstrated with high efficiency of 80% around 825 nm [9]. Full color metasurface holograms have been reported over wide bandwidth with high imaging quality [10, 11]. Improved retrieval method is used to increase the field of view and to reduce the

background noises [12, 13]. Metasurface holograms operating in the terahertz (THz) band have been extensively studied as well [8, 14]. Imaging with high signal-to-noise ratio is achieved using metallic C-shaped [15] or dielectric metasurfaces [16] with independent control of amplitude and phase. Polarization-multiplexed [17] and frequency-multiplexed [18] holograms further increase the data storage capability.

The above metasurfaces can be classified as metallic holograms and high-index dielectric holograms, where the metallic designs often work in the reflection mode to ensure high efficiency, and the high-index dielectric ones enable efficient wavefront shaping in the transmission mode with minimum coupling among neighboring elements. For THz operation, the accessible high-index low-loss dielectric is limited to silicon. Deep silicon etching is usually required with cycles of etching and protection steps during the preparation of the metasurfaces, which may affect the sidewall roughness and verticality, and limit the applications in lower THz frequencies.

In contrast, there are plenty of low-index polymers transparent for THz waves with refractive indices around 1.5 to 2 [19], such as polyactic acid (PLA), polypropylene (PP), polystyrene (PS), which can be shaped into complicated structures using the 3D printing technique [20]. 3D-printed bulk elements, such as waveguides [21, 22], antennas [23], convex lenses [19, 24, 25], spiral and axicon phase plates [26] have been proven as THz functional devices with the merit of low cost and fast fabrication speed. Metasurfaces based on 3D-printed polymers are less reported and more challenging as high resolution is needed to resolve the subwavelength texture. Additionally, the effect of the undesired coupling between low-index elements on the performance of wavefront shaping is unknown.

In this study, we propose a 3D-printed metasurface for holographic imaging at the low THz frequency 0.14 THz. The design process is detailed. The experimental characterization of the metasurface shows a good agreement with the simulation results. The image is reconstructed with good fidelity. The study here not only provides a cost-effective way to develop THz holography, but also offers a general method for metasurface wavefront shaping using low-index dielectric widely existing in any frequency band.

2. Design of the metasurface hologram using PLA

As shown in Figure 1(a), the metasurface is composed of dielectric rectangular rods, whose dimensions are carefully chosen to reshape the incident y-polarized plane wave into an N shape at a distance of 50 mm. The material of the metasurface is chosen as PLA, which is one of the most commonly used 3D printing raw material based on the fused deposition modeling technology. Before the design of the elements, we 3D print a slab and test the dielectric constant of PLA in the THz time-domain spectroscopy (THz-TDS) system. The real part of the dielectric constant is stable over a wide frequency band, and the imaginary part increases with the

frequency. At the target frequency 0.14 THz , the THz-TDS system does not give confident data due to the low signal-to-noise ratio. Considering the low dispersion of the dielectric, the dielectric constant of PLA is determined as 1.57 at 0.14 THz .

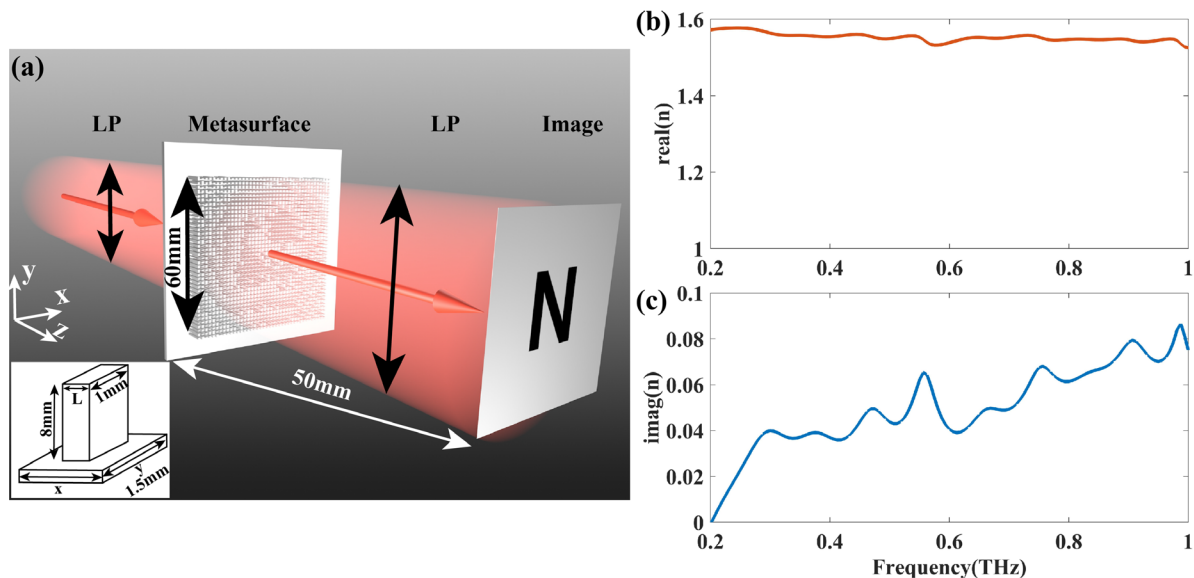


Fig. 1 (a) Schematic illustration of the metasurface holography at the low terahertz frequencies. The inset shows an element of the metasurface with geometrical parameters marked. (b-c) The dielectric constant of PLA measured by the THz-TDS system. The real part is shown in (b) and the imaginary part in (c).

As shown by the inset of Figure 1(a), the element is a rectangular rod on the substrate. The period of the element is 1.5 mm along x and y directions. The thickness of the substrate is set as 1 mm for support. The height of the rod is 8 mm . All the rods have the same width, which is 1 mm . The length L is a variable to obtain different phase delays. The variation of the transmission amplitude and phase with the length L is shown in Figure 2. The calculation is done in Lumerical FDTD by setting periodic boundary conditions in x and y directions and perfectly matched layers in z direction with y -polarized plane wave excitation. As can be seen from Figure 2(a) and 2(b), the phase can be tuned over a 2π range by changing L from 0.2 mm to 1.3 mm , while the amplitude is always above 0.96 . Once the phase hologram is retrieved, the elements with proper L can be arranged into the desired locations to form the metasurface hologram.

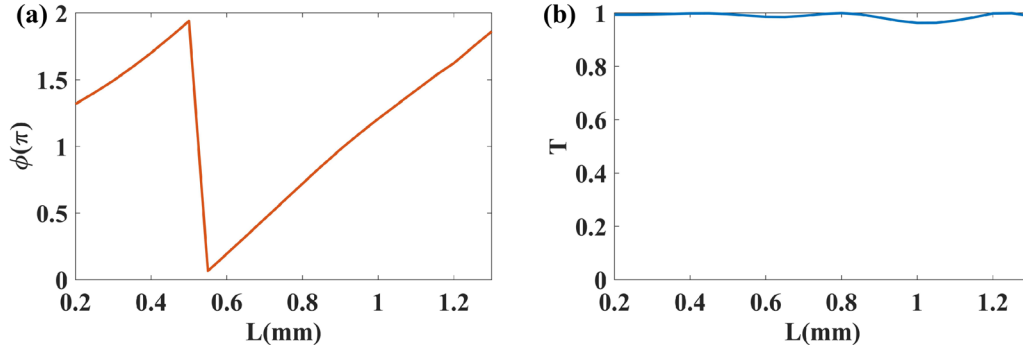


Fig. 2 Transmission phase (a) and amplitude (b) of the rectangular bar in a periodic array when the length L is varied.

3. Fabrication and experiment

We next use the Gerchberg-Saxton (GS) algorithm [27, 28] to retrieve the phase hologram. The phase distribution is calculated iteratively using the Rayleigh-Sommerfeld diffraction formula [14]. For each iteration, two diffracted waves propagating along the opposite directions are calculated by considering the image as a source and the metasurface as a source, respectively. The amplitude in the metasurface plane is replaced by a unity distribution for phase-only hologram, and the amplitude in the image plane is replaced by the target amplitude distribution during the iteration. The phases in the two planes are updated until the amplitude in the image plane before the replacement is converged to the target one. Figure 3(a) shows the calculated phase hologram for a target image of letter N at a distance 50 mm after the metasurfaces. Combining Figure 2 and Figure 3(a), one can determine the dimensions of the rods inside the metasurface so that they can best implement this phase distribution. The structure of the metasurface is shown in Figure 3(b). The size is $61\text{ mm} \times 61\text{ mm}$. It contains 41×41 rods. All the rods have the same dimension along y and variable dimension along x .

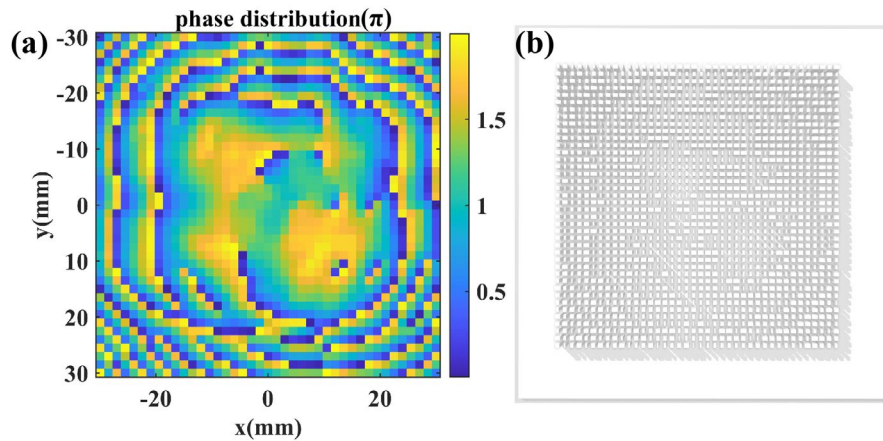


Fig. 3 (a) The desired phase distribution in the metasurface plane calculated from the GS algorithm for reconstruction of a letter N 50 mm away. (b) The metasurface structure assembled by properly choosing the length of the rods according to the phase in Fig. 2(a).

The metasurface is fabricated using a 3D printer (Raise 3D N2). The nozzle with diameter of 0.2 mm is heated to 215°C to melt the PLA filament and to additively shape it into the desired structure according to advanced motion control. The printing speed is 60 mm/s . The time consumed for printing this metasurface is 15 hours. Top view and side view of the sample are shown in Figure 4. The inset in Figure 4(a) shows a zoomed view inside the square area, where rods with different dimensions can be well resolved. When the rod has a very small length L , it may have some connection with the neighboring element. But after the measurement, it turns out that such imperfection does not have significant effect on the image quality.

The experimental setup for measuring the image intensity is shown in Figure 5(a). A continuous-wave IMPATT diode with radiation frequency of 0.14 THz is used as the source. The beam is collimated by a Teflon convex lens with a focal length of 151 mm and a diameter of 4 inches . After collimation, the source is a quasi-gaussian distribution with the beam waist of 25 mm . A polarizer is inserted before the metasurface to ensure y -polarized excitation. After the metasurface, a Schottky diode detector is mounted on a three-dimensional translation stage to measure the intensity distribution with a step of 1 mm .

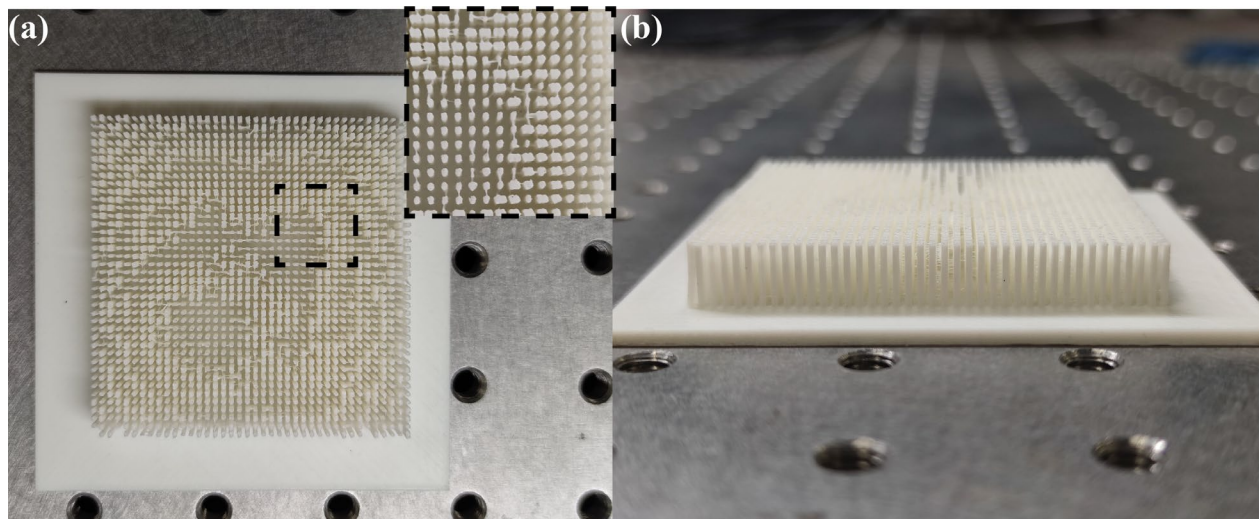


Fig. 4 (a) Top view of the 3D-printed metasurface hologram. The detailed structures within the square is zoomed in the inset for clarity. (b) Side view of the 3D-printed metasurface hologram.

The measured intensity at a distance of 50 mm from the metasurface is shown in Figure 5(d). It shows the desired N shape. For better comparison, some theoretical and numerical calculations are done. Figure 5(b) is the theoretical prediction of the image intensity based on the Rayleigh-Sommerfeld diffraction equation when the field in the metasurface plane has unity amplitude and the desired phase profile in Figure 3(a). It shows the best image quality that the metasurface could possibly achieve. When the whole metasurface in Figure 3(b) is exactly

modelled in the simulation, the intensity becomes Figure 5(c). Due to the element discretization and the deviation from the perfect periodic environment, the image quality is worse than the theoretical one. But it is still easy to recognize the letter N. Interestingly, the simulated and measured intensities in Figure 5(c) and 5(d) show very high similarity, demonstrating that the fabrication imperfection is not large enough to deteriorate the optical response. We further define the image efficiency as the ratio between the power distributed in the letter N and the total power in the imaging plane. The image efficiency is 94.19%, 70.74% and 65.68% in Figure 5(b-e), respectively.

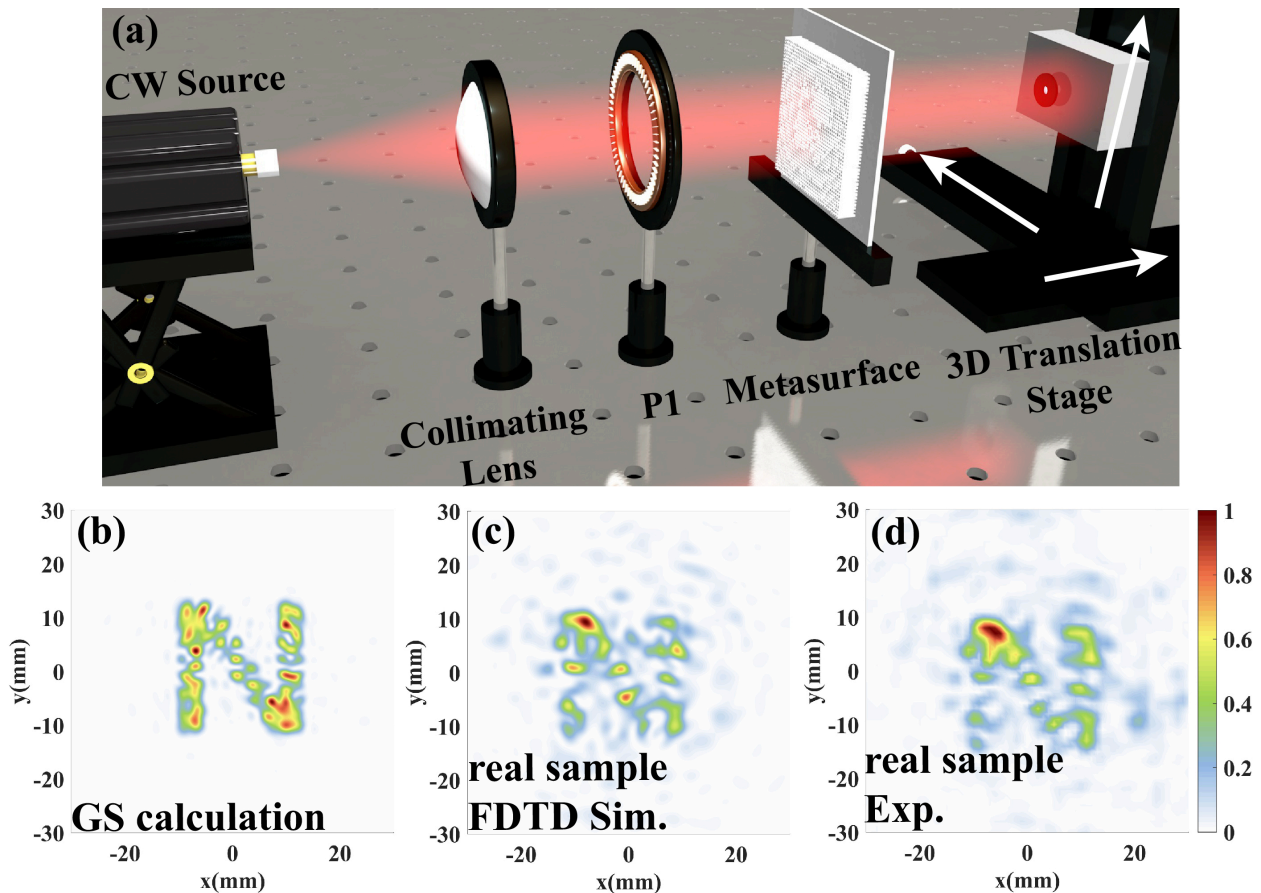


Fig. 5 (a) The experimental setup for characterization of the metasurface hologram. (b) The ideal image pattern based on GS calculation. (c) FDTD simulation of the image through the real metasurface model. (d) Experimentally measured image intensity through the metasurface.

4. Conclusions

A terahertz metasurface hologram made of 3D-printed low-index polymer rods is designed and experimentally tested at 0.14 THz. The phase hologram is calculated based on the Rayleigh-Sommerfeld diffraction theory and the Gerchberg-Saxton algorithm. The printed

sample reconstructs the image of a letter N at the desired position with high fidelity. Highly consistent intensity distributions are observed between the simulation and the measurement. The study here indicates that low-index dielectric metasurfaces can be used for complex wavefront shaping, and 3D printing offers a low-cost and efficient way to build functional THz metadevices.

Funding

This work was supported by National Natural Science Foundation of China (61805123, 61831012, 62175118); National Key Research and Development Program of China (2017YFA0701000).

References

- [1] D. GABOR. “A New Microscopic Principle”. *Nature*, 161, 777–778 (1948).
- [2] E. N. Leith and J. Upatnieks. “Wavefront Reconstruction with Diffused Illumination and Three-Dimensional Objects”. *J. Opt. Soc. Am.*, 54, 1295–1301 (1964).
- [3] A. W. Lohmann and D. P. Paris. “Binary Fraunhofer Holograms, Generated by Computer”. *Appl. Opt.*, 6, 1739–1748 (1967).
- [4] A. Kozma and D. L. Kelly. “Spatial Filtering for Detection of Signals Submerged in Noise”. *Appl. Opt.*, 4, 387–392 (1965).
- [5] L. B. Lesem, P. M. Hirsch, and J. A. Jordan. “The Kinoform: A New Wavefront Reconstruction Device”. *IBM J. Res. Dev.*, 13, 150–155 (1969).
- [6] Q. Jiang, G. Jin, and L. Cao. “When metasurface meets hologram: principle and advances”. *Adv. Opt. Photonics.*, 11, 518–576 (2019).
- [7] L. Huang, S. Zhang, and T. Zentgraf. “Metasurface holography: from fundamentals to applications”. *Nanophotonics.*, 7, 1169–1190 (2018).
- [8] J. He, T. Dong, B. Chi, et al.. “Metasurfaces for Terahertz Wavefront Modulation: a Review”. *J. Infrared, Millimeter, Terahertz Waves.*, 41, 607–631 (2020).
- [9] G. Zheng, H. Mühlenbernd, M. Kenney, et al.. “Metasurface holograms reaching 80% efficiency”. *Nat. Nanotechnol.*, 10, 308–312 (2015).
- [10] Y. Hu et al.. “3D-Integrated metasurfaces for full-colour holography”. *Light Sci. Appl.*, 8, 86 (2019).
- [11] L. Xiong et al.. “Multicolor 3D meta-holography by broadband plasmonic modulation”. *Sci. Adv.*, 2, e1601102 (2021).
- [12] Y. Mu, M. Zheng, J. Qi, et al.. “A large field-of-view metasurface for complex-amplitude hologram breaking numerical aperture limitation”. *Nanophotonics.*, 9, 4749–4759 (2020).

- [13] A. C. Overvig et al. "Dielectric metasurfaces for complete and independent control of the optical amplitude and phase". *Light Sci. Appl.*, 8, 92 (2019).
- [14] X. Liu et al. "Metasurface-based computer generated holography at terahertz frequencies". *Opto-Electronic Eng.*, 47, 190674 (2020).
- [15] Q. Wang et al. "Broadband metasurface holograms: toward complete phase and amplitude engineering". *Sci. Rep.*, 6, 32867 (2016).
- [16] Q. Wang et al. "All-Dielectric Meta-Holograms with Holographic Images Transforming Longitudinally". *ACS Photonics.*, 5, 599–606 (2018).
- [17] Q. Wang et al. "Reflective chiral meta-holography: multiplexing holograms for circularly polarized waves". *Light Sci. Appl.*, 7, 25 (2018).
- [18] Q. Wang et al. "Polarization and Frequency Multiplexed Terahertz Meta-Holography". *Adv. Opt. Mater.*, 5, 1700277 (2017).
- [19] S. F. Busch, M. Weidenbach, M. Fey, et al. "Optical Properties of 3D Printable Plastics in the THz Regime and their Application for 3D Printed THz Optics". *J. Infrared, Millimeter, Terahertz Waves.*, 35, 993–997 (2014).
- [20] B. Zhang, Y.-X. Guo, H. Zirath, et al. "Investigation on 3-D-Printing Technologies for Millimeter- Wave and Terahertz Applications". *Proc. IEEE.*, 105, 723–736 (2017).
- [21] S. Pandey, B. Gupta, and A. Nahata. "Terahertz plasmonic waveguides created via 3D printing". *Opt. Express.*, 21, 24422–24430 (2013).
- [22] M. Weidenbach et al. "3D printed dielectric rectangular waveguides, splitters and couplers for 120 GHz". *Opt. Express.*, 24, 28968–28976 (2016).
- [23] P. T. Timbie, J. Grade, D. van der Weide, et al. "Stereolithographed MM-wave corrugated horn antennas". in *2011 International Conference on Infrared, Millimeter, and Terahertz Waves.*, 1–3 (2011).
- [24] A. D. Squires, E. Constable, and R. A. Lewis. "3D Printed Terahertz Diffraction Gratings And Lenses". *J. Infrared, Millimeter, Terahertz Waves.*, 36, 72–80 (2015).
- [25] F. Zhou, W. Cao, B. Dong, et al. "Additive Manufacturing of a 3D Terahertz Gradient-Refractive Index Lens". *Adv. Opt. Mater.*, 4, 1034–1040 (2016).
- [26] X. Wei et al. "Generation of arbitrary order Bessel beams via 3D printed axicons at the terahertz frequency range". *Appl. Opt.*, 54, 10641–10649 (2015).
- [27] C. Chang, J. Xia, L. Yang, et al. "Speckle-suppressed phase-only holographic three-dimensional display based on double-constraint Gerchberg-Saxton algorithm". *Appl. Opt.*, 54, 6994–7001 (2015).
- [28] A. V. Zea, J. F. Barrera Ramirez, and R. Torroba. "Optimized random phase only holograms". *Opt. Lett.*, 43, 731–734 (2018).